Control Engineering Practice 175 (2026) 107113

Contents lists available at ScienceDirect

Control Engineering Practice

journal homepage: www.elsevier.com/locate/conengprac

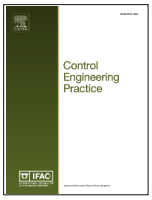

Integrating rule awareness and semantic reasoning in collision-free vessel path planning

Nikos Kougiatsos *, Abhishek Dhyani , Vasso Reppa

Department of Maritime and Transport Technology, Delft University of Technology, Mekelweg 2, Delft, 2628CD, South Holland, the Netherlands

ARTICLE INFO

Keywords:
AI and embodied-AI in marine systems
Guidance, navigation and control
Semantics
Collision avoidance
Autonomous surface vehicles (ASVs)

ABSTRACT

This paper presents the design of an intelligent guidance framework for collision-free navigation of Autonomous Surface Vessels (ASVs), integrating traffic rule awareness and reasoning characteristics. The proposed framework leverages the available qualitative information related to traffic rules and the operational environment(s), in the form of semantic information, as well as sensor information to make online path planning decisions. A modular finite-state machine assigns traffic roles, while the path planner computes a collision-free envelope and reasons over a path, considering both vessels and infrastructure. A Line-of-Sight algorithm and controller enforce the selected path. The method's effectiveness is demonstrated in a multi-environment case study involving head-on and crossing encounter scenarios, showcasing its adaptability and efficiency across short-sea and inland waterway operations.

1. Introduction

Nowadays, waterborne transport is responsible for more than 80 % of global cargo services (Pratson, 2023). In an effort to realise the European's Green Deal's target of climate-neutrality by 2050, the shift from road transport to inland waterways and the automation of multi-modal mobilities have been identified as two of the European Union's thematic priorities (Smeds & Cavoli, 2021). Autonomous Surface Vessels (ASVs) have emerged as a popular research topic within this context due to their potential to reduce operational costs, enhance traffic flow and improve navigational safety. Among navigational safety risks, collision events are the most prominent, representing 36 % of vessel casualties in 2023, as recorded by the European Maritime Safety Agency (2024). The recorded casualty events incorporate both collisions with the surrounding infrastructure (e.g., banks, bridges, locks) and other vessels.

Motion planning and control are essential functionalities in ASV applications, and are usually handled by a dedicated Guidance, Navigation and Control (GNC) system. The guidance system is primarily responsible for planning collision-free paths, considering the operational environment of the ASV (e.g., Inland waterways, short sea) and its associated spatial constraints (e.g., water depth, bank effects) that influence the dynamic behavior of the vessel (Zhang et al., 2025). In addition, different traffic rules apply to different types of environments and should be transcribed in the design of the guidance system. To efficiently integrate and reason over the knowledge required for safe ship guidance under different and potentially challenging encounter scenarios, Artificial Intelligence methods are increasingly applied (Luo et al., 2022).

In Yang et al. (2019), a cooperative collision avoidance mechanism is developed for a network of vessels. The online path planning for each vessel involves a selection from a set of possible routes with different characteristics (e.g., closest time of approach between vessels) through the application of a genetic algorithm. Nonetheless, the authors only consider vessel to vessel collisions in their study, excluding collisions with the infrastructure. The authors of Hinostroza et al. (2021) consider the risk of collision with static obstacles and propose a guidance scheme targeted at path planning and the calculation of the reference heading signal, through a Line-of-Sight (LOS) guidance law. The deviation of the reference path is selected through an optimization process, similar to Dijikstra's algorithm, called the Fast Marching method. Li et al. (2023) in their work consider both static and dynamic obstacles. The optimal path deviation to avoid collisions is selected through the formulation of vessel speed and distance constraints in a robust optimisation framework. While these papers contribute significantly in the calculation process of the optimal deviation from the original route to avoid collisions, most of the proposed algorithms are associated with high complexity and can prove computationally intensive in heavy traffic scenarios. To handle this complexity, He et al. (2022, 2025), Zhou et al. (2021) employ the Velocity Obstacle (VO) method for collision avoidance. VO optimises the generated path deviation based on information about the own vessel's course and position, the other vessel's

* Corresponding author.
E-mail addresses: n.kougiatsos@tudelft.nl (N. Kougiatsos), a.dhyani-1@tudelft.nl (A. Dhyani), v.reppa@tudelft.nl (V. Reppa).

https://doi.org/10.1016/j.conengprac.2026.107113
Received 2 November 2025; Received in revised form 5 June 2026; Accepted 6 June 2026
Available online 11 June 2026

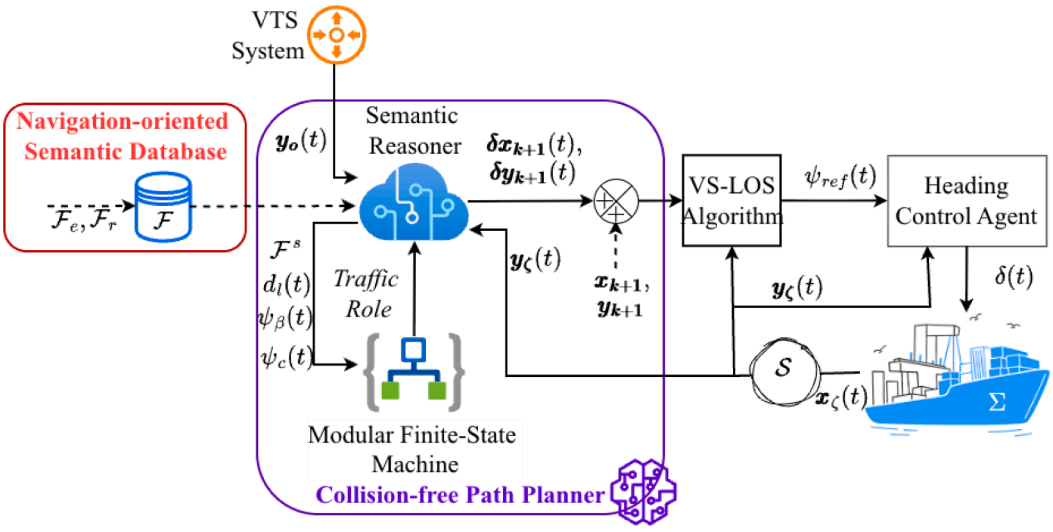

Fig. 1. Proposed Guidance Framework. Dashed arrows are used for signals that are provided offline while continuous arrows signify the online flow of information. The contributions of this paper are highlighted with colored/ curved boxes.

position and velocities and the safe distance between vessels. The computational burden associated with the optimisation process is addressed by a pseudo-algorithm, though the implementation aspects of obtaining and using the information about other vessels and obstacles are left out of the discussion. Zhou et al. (2022), instead propose stream functions to calculate the course deviation for collision avoidance, inspired by the field of hydrodynamics. Nevertheless, the previous methods consider that both the position and the velocities of other vessels are known, excluding details on how this information is obtained. Regarding learning-based methods, Deep Reinforcement learning algorithms for vessel to vessel collision avoidance are investigated in single and cooperative AI agent settings in Yoshioka and Hashimoto (2022), Yoshioka et al. (2024). Positive and negative rewards are assigned when the vessel follows the waypoints, enters defined dangerous areas for collision, and performs according to the traffic rules. The assignment of the traffic roles to the involved vessels is left out of the discussion though in these papers. The majority of reviewed literature focuses on the integration of the Convention on the International Regulations for Preventing Collisions at Sea (COLREGs) (International Maritime Organization (IMO), 1972) in the guidance system. Meanwhile, regional regulations applicable to Inland Waterway traffic, such as the Binnenvaartpolitiereglement (BPR) (Overheid.nl, 2025) and the Police Regulations for the Navigation of the Rhine (RPR) (CCNR, 2024) have not been adequately discussed (Tran et al., 2025) for the same purpose.

In this research work, an intelligent guidance framework is designed, incorporating rule awareness and reasoning characteristics, to ensure the collision-free navigation of marine vessels. The overall framework is illustrated in Fig. 1. More specifically, this paper examines changes in the type of environment, and the subsequent switching between applicable traffic rules. Rule awareness relies on the qualitative modelling of applicable traffic rules and operational environment characteristics in a computer-cognitive format, using semantics in $\mathcal{F}$, before the start of the operation. The path planner is designed to avoid collisions with both other vessels (dynamic obstacles) and the surrounding infrastructure (static obstacles). To this end, a semantic reasoner is incorporated, leveraging both the semantic information and sensor feedback from the own vessel sensors and from other vessels (e.g., via the Vessel Traffic System (VTS)), to make well-informed decisions on the applicable traffic rules and environment, as well as the required reference path deviation to avoid collisions. The calculation of the reference path deviation relies on the derivation of geometrical conditions, without requiring information on the vessel velocities. The reasoner is assisted by a modular Finite-State Machine (FSM) approach, considering both COLREGs and other regional rules, for the classification of the encounter scenario and the assignment of the traffic role. Tracking of the modified reference path is accomplished through the use of an already-developed LOS guidance law (Kougiatsos & Reppa, 2026) and applied using a PID controller, tracking the provided heading reference. A well-established 3-DoF First-Principle model Σ, provided by the Maneuvering Modelling Group (MMG), is used for simulation purposes.

Previous work of the authors (Tsolakis et al., 2024) focused on the translation of COLREG requirements using a Finite-State Machine Approach. However, regional traffic rules were left out of the discussion. Kougiatsos et al. (2025) semantically described and reasoned between different topology and control design choices for marine vessels. Though, the semantic translation and reasoning between regulations was not considered. Finally, Kougiatsos and Reppa (2026) developed a Virtual-sensor informed LOS guidance law, shown in Fig. 1, for the adaptive estimation of both sensor faults and the unknown sideslip angle. Nonetheless, collision avoidance objectives were not explored in this work.

The main contribution of this paper is the development of an intelligent collision-free path planner (Section 4) that utilizes the available sensor and semantic information to make decisions on the applicable traffic rules and environment characteristics and reasons over a safe path envelope to avoid collisions. The consideration of the infrastructure for collision avoidance allows for safe vessel operation in restricted waterways. The modular Finite-state machine approach allows for the consideration of multiple traffic rules, dictating different behavior for the vessel. As a result, the vessel operation (Section 2) can safely adapt to different operational environments. The translation of traffic rules as part of the semantic database, in Section 3, facilitates the collaboration between of the relevant regulatory bodies and engineers for the design of the collision avoidance system. Simulation results from the application of the proposed methodology in head-on and crossing scenarios, occurring between a short-sea and an inland waterway environment are used to verify the applicability and efficiency of the method, in Section 5. Finally, concluding remarks are provided in Section 6.

2. Problem formulation

We assume that the ASV moves in a workspace $\mathcal{W} \subseteq \mathbb{R}^2$. Similar to Zhang et al. (2025), we use the MMG model formulation. To this

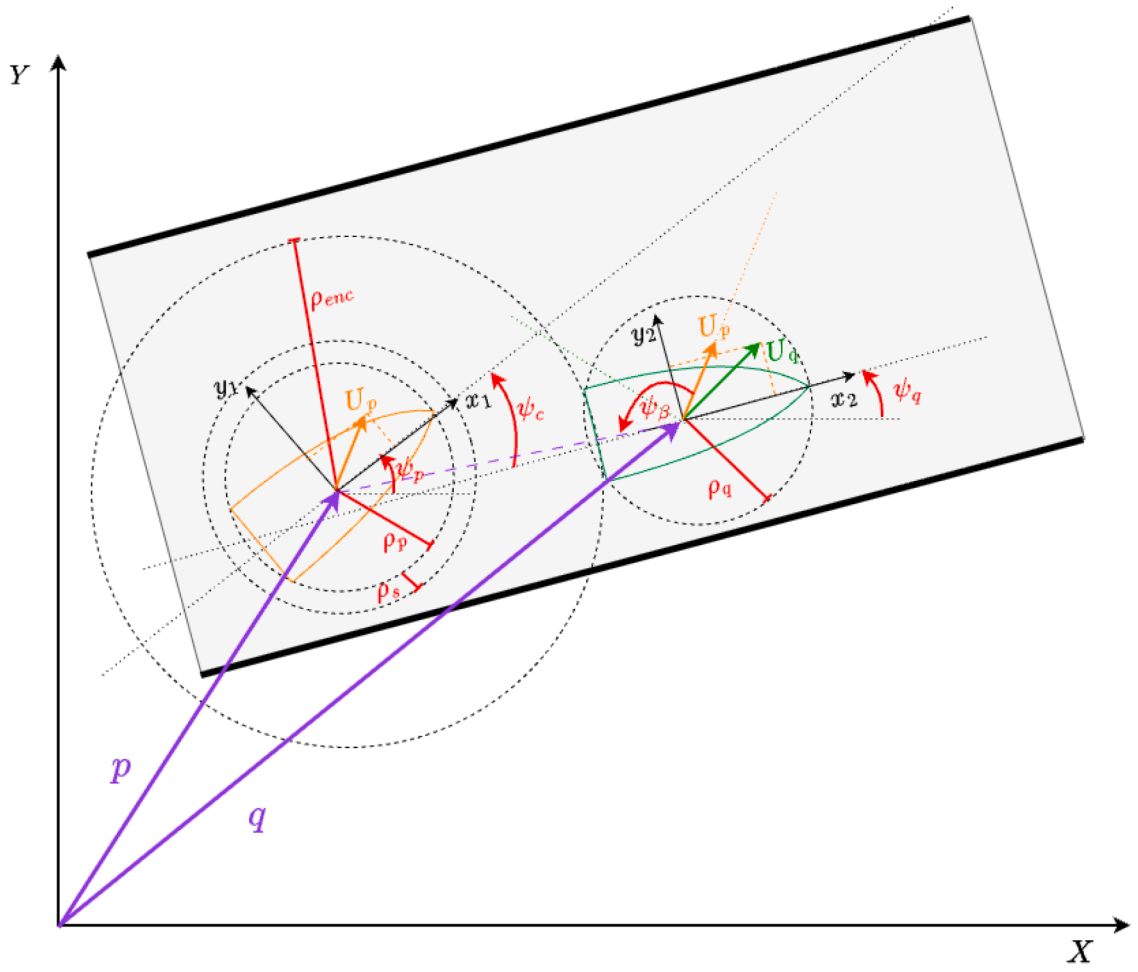

Fig. 2. Encounter situation analysis between own (orange) and an encountered other vessel (green) while moving through restricted waters. The basic geometrical characteristics of the planar motion in the plane X-Y are shown. (For interpretation of the references to colour in this figure legend, the reader is referred to the web version of this article.)

end, the ASV's configuration is described by its planar position state $(x(t), y(t), \psi(t))^\top \in \mathbb{R}^3$, its longitudinal and lateral velocities $u(t) \in \mathbb{R}$ and $v(t) \in \mathbb{R}$ and its yaw rate $r(t) \in \mathbb{R}$. The overall state of the vessel is denoted as $\boldsymbol{x}(t) = (x(t), y(t), \psi(t), u(t), v(t), r(t))^\top \in \mathbb{R}^6$ and the control input to the vessel as $\boldsymbol{u}(t) = \delta(t) \in \mathcal{U} \subseteq \mathbb{R}$, where $\delta(t)$ represents the rudder angle.

Assuming a coordinate system with its center at the origin of the vessel's local coordinate system, the evolution of the ASV's state is described by the following nonlinear differential equations:

$$\Sigma : \dot{\boldsymbol{x}}_{\boldsymbol{\zeta}}(t) = \begin{bmatrix} \cos(\psi) & -\sin(\psi) & 0 & 0 & 0 & 0 \\ \sin(\psi) & \cos(\psi) & 0 & 0 & 0 & 0 \\ 0 & 0 & 1 & 0 & 0 & 0 \\ 0 & 0 & 0 & \frac{1}{(m+m_x)} & 0 & 0 \\ 0 & 0 & 0 & 0 & \frac{I_z + x_G^2 m + J_z}{C_{y\psi}} & -\frac{x_G m}{C_{y\psi}} \\ 0 & 0 & 0 & 0 & -\frac{x_G m}{C_{y\psi}} & \frac{(m+m_x)}{C_{y\psi}} \end{bmatrix} \cdot \begin{bmatrix} u \\ v \\ r \\ (m+m_y)v_m r + x_G m r^2 + X_H(\boldsymbol{x}_\zeta) + X_P(\boldsymbol{x}_\zeta) + X_R(\boldsymbol{x}_\zeta, \boldsymbol{u}) \\ Y_H(\boldsymbol{x}_\zeta) + Y_R(\boldsymbol{x}_\zeta, \boldsymbol{u}) + \sigma_b Y_B(\boldsymbol{x}_\zeta) + (m+m_x)ur \\ N_H(\boldsymbol{x}_\zeta) + N_R(\boldsymbol{x}_\zeta, \boldsymbol{u}) + \sigma_b N_B(\boldsymbol{x}_\zeta) - x_G mur \end{bmatrix}, \tag{1}$$

where $C_{y\psi} = (m+m_x)(I_z + x_G^2 m + J_z) - (x_G m)^2$, m is the mass of the vessel, m_x and m_y denote the added mass in the longitudinal and transverse directions, I_z is the moment of inertia and J_z denotes the added moment of inertia, x_G is the longitudinal position of the center of gravity, v_m expresses the sway velocity at midship, and $\sigma_b \in \{0, 1\}$ is a parameter explained in the Section 3. The hull forces X_H (surge direction), Y_H (sway direction) and yaw moment N_H, the rudder forces X_R (surge direction), Y_R (sway direction) and yaw moment N_R, the bank forces Y_B (sway direction) and yaw moment N_B, and the propeller force X_P compose the sums in the right hand side of (1). Note that the influence of the state $\boldsymbol{x}$ of the vessel and the control input $\boldsymbol{u}$ in the calculation of the forces acting on the vessel is explicitly stated in (1). The modeling of the vessel hydrodynamic forces is discussed in Zhang et al. (2025). The vessel incorporates a set of sensors $\mathcal{S}$ described as:

$$\mathcal{S} : \boldsymbol{y}_\zeta(t) = [x, y, \psi]^\top, \tag{2}$$

where $\boldsymbol{y}_\zeta \in \mathbb{R}^3$ denotes the sensor values.

During navigation, the ASV's path planning decisions are influenced by (i) the sensor feedback from $\mathcal{S}$ (quantitative), (ii) the information communicated from other traffic participants (e.g., using VTS) (quantitative), and (iii) the applicable traffic rules to be respected for collision avoidance (qualitative). The goal of this paper is to develop an intelligent guidance framework for ASVs that is aware of traffic rules, is able to reason using the available quantitative and qualitative knowledge for collision avoidance, and can plan a set of collision-free paths.

3. Navigation-oriented semantic database

The backbone of the proposed guidance framework is a navigation-oriented Semantic database. Similar to our previous work in Kougiatsos et al. (2025), the database $\mathcal{F}$ can be defined as:

$$\mathcal{F} = \mathcal{F}_e \cup \mathcal{F}_r, \tag{3}$$

where $\mathcal{F}_e$ stores the semantic information related to the vessel's "operational environment", and $\mathcal{F}_r$ stores the semantic information related to the "traffic rules" that the vessel should follow. These are defined as follows:

"Operational environment": During the vessel's mission, the type of operational environment dictates the physical infrastructure limitations that the vessel is required to take into account (e.g., waterway width w and water depth d). An "operational environment" can be thus expressed by the parameters w and d, as well as a bank force switching variable $\sigma_b \in \{0, 1\}$, implemented in the right half side of Eq. (1).

"Traffic Rules": Depending on the location where the vessel operates, certain rules will dictate its traffic behavior. These rules can be generally categorized in three categories, the "Situation Invariant Rules", "Situation Analysis Rules" and "Situation Dependent Rules". The first are always followed regardless of the traffic scenario. A vessel can assume one of the following three roles in an encounter situation with another vessel; Stand On (when expected to keep the same course and speed), Give-way (when expected to take collision avoidance action) and Emergency Give-way (in situations when the Stand-On vessel finds herself so close to collision and is expected to take any action to aid in avoiding said collision). "Situation Analysis Rules" are used to assign the role $r \in \{1, 2, 3\}$ (1: give-way, 2: stand-on and 3: emergency give-way) of the vessel in the specific encounter scenario. "Situation Dependent Rules" are used to dictate a safe distance ρ_s from other vessels, a safe lane distance d_l and a safe speed U_s for the own vessel, depending on r.

The collision-free path planner presented next considers the safe distances to perform decisions on the safe path deviation to avoid collision. The safe speed constraint, though important, requires the consideration of velocity measurements in (2) and of speed as part of the control objectives. As such, it is left out of the scope of the present research work.

4. Collision-free path planner

The collision-free path planner module presented in this section involves the design of two cyber agents, the semantic reasoner and the modular FSM. Semantic reasoning aims at effectively utilizing the available semantic information stored in the database $\mathcal{F}$ for online operational decisions (Kougiatsos et al., 2025). The reasoner is responsible for the assessment of the encounter conditions, the decision on the applicable traffic rules and the planning of a collision-free path. To accomplish the third task, the semantic reasoner is assisted by a modular Finite-State Machine, mapping the calculated encounter parameters to specific traffic roles.

4.1. Semantic reasoner

The assessment of the encounter conditions typically involves performing several geometrical calculations using the inputs from sensors in S to assess quantities such as the relative bearing and relative heading between the own and other vessels, the distance between the own and other vessel(s) d and the distance between the own vessel and the bank in case of inland waterway navigation (d_l). Based on the various applicable traffic rules (i.e., COLREGS, BPR, PRR), "ample time" should be allowed to make decisions related to collision avoidance, while the vessels are expected to "keep well clear" of each other. These requirements geometrically translate to an encounter distance ρ_{enc}, used to initiate the assessment of the encounter situation when other vessels are in range of this radius, and a safe distance ρ_s, used to enforce the vessels to keep well clear of each other. Moreover, a vessel radius $\rho_p = L/2$ and $\rho_q = L'/2$ is prescribed for the own and other vessel, respectively, where L, L' denote the lengths of the own and the other vessel, respectively. While a circular ship domain choice is made in this paper, non-circular shapes can also be used for the semantic reasoner. The relative bearing ψ_β is used to characterize the relative position between the two vessels, while the relative heading ψ_c characterizes the difference in the heading of the two vessels. The main geometrical parameters of the encounter scenario between the own and another vessel can be seen in Fig. 2, while the formulas used for the calculation of ψ_β, ψ_c can be found in Tsolakis et al. (2024).

The selection of the applicable traffic rules from the semantic database takes the form of a mapping using the GPS signal measurement, as follows:

$$\mathcal{Y}_{GPS} \times \mathcal{F} \mapsto \mathcal{F}^s, \tag{4}$$

where $\mathcal{Y}_{GPS}$ denotes the space of GPS sensor measurements and

$$\mathcal{F}^s = \mathcal{F}_e^s \cup \mathcal{F}_r^s \subseteq \mathcal{F} \tag{5}$$

denotes the active part of the semantic database for the current environment ($\mathcal{F}_e^s \subseteq \mathcal{F}_e$) and applicable traffic rules ($\mathcal{F}_r^s \subseteq \mathcal{F}_r$).

In cases where the own vessel assumes a Give-Way or an Emergency Give-Way role, appropriate action needs to be taken to avoid collisions. In the context of this paper, the appropriate action to avoid collisions is the modification of the vessel's reference waypoints, produced by the global planner before the start of the mission. This change occurs during operation and is implemented in discrete time steps using the same sampling rate as the controller until the encounter situation is resolved.

Let us assume a constant reference path provided at the start of the mission, and discretized in waypoints $k = 0, 1, \dots, n$, denoted as $(x_k, y_k)^\top$. We modify the waypoints $k+1$ at each time t using the terms $(\delta x_{k+1}(t), \delta y_{k+1}(t))^\top$, so that the new path is defined as (Ali et al., 2024):

$$x'_{k+1}(t) = x_{k+1} + \delta x_{k+1}(t), \tag{6}$$

$$y'_{k+1}(t) = y_{k+1} + \delta y_{k+1}(t), \tag{7}$$

where $x'_{k+1}(t)$ and $y'_{k+1}(t)$ denote the coordinates of the modified reference path.

4.1.1. Collisions with other vessels

If the current position $(x_{o,i}, y_{o,i})^\top$ and heading $\psi_{o,i}$ of each of the other vessels i ($i = 1, 2, \dots, n_v$) is known, where n_v denotes the total number of the other vessels, similar to Johansen et al. (2016), we assume that its movement until the following time step t is constrained on a line:

$$\mathcal{E}_i : \begin{cases} x'_{o,i}(a) = x_{o,i} + a\cos(\psi_{o,i}), \\ y'_{o,i}(a) = y_{o,i} + a\sin(\psi_{o,i}), \end{cases} \tag{8}$$

where $a \in (-\infty, \infty)$ is the path parameter, $(x'_{o,i}, y'_{o,i})^\top$ denote the set of positions that the other vessel is expected to occupy until the next time step t, based on the current knowledge of its position and heading. For each of the new future waypoints $k+1$ of the own vessel, we calculate its distance from each $\mathcal{E}_i$ according to the following formula:

$$d_{W\mathcal{E}_i}(t) = \left| -sin(\psi_{o,i})\left(x'_{k+1}(t) - x_{o,i}\right) + cos(\psi_{o,i})\left(y'_{k+1}(t) - y_{o,i}\right) \right|, \quad \forall i \in \{1, 2, \dots, n_v\}. \tag{9}$$

In order to guarantee a vessel-to-vessel collision-free path, our vessel should maintain a safe distance ρ_s from every other vessel that allows for "ample time for decision-making", meaning that:

$$d_{W\mathcal{E}_i}(t) \geq \rho_s + \rho_p + \rho_q. \tag{10}$$

Substituting (6), (7), (9) in (10) and after some algebraic manipulations, the following set of constraints is obtained for collision avoidance with every other vessel i:

$$\left|\delta y_{k+1}\cos(\psi_{o,i}) - \delta x_{k+1}\sin(\psi_{o,i})\right| \geq \left(\rho_s + \rho_p + \rho_q\right) + \left|(y_{o,i} - y_{k+1})\cos(\psi_{o,i}) + (x_{k+1} - x_{o,i})\sin(\psi_{o,i})\right|, \forall i \in \{1, \dots, n_v\}. \tag{11}$$

4.1.2. Collisions with infrastructure

For inland waterway operations, collision avoidance with the banks of the waterway demands that a certain safe distance needs to be respected. For instance, Rule 9 of COLREGS dictates that "A vessel proceeding along the course of a narrow channel or fairway shall keep as near to the outer limit of the channel or fairway which lies on her starboard side as is safe and practicable […]".

Let us define w, $(x, y) \mapsto w$, as the non-constant but known waterway width, dependent on the planar coordinates of our vessel, and s_w as a safety factor defining the safe distance from the bounds of the canal and receiving values in $[0, 0.5)$. This factor serves as a heuristic, and its value can be set for limiting vessel-to-bank interactions (Lataire et al., 2018). Assuming that the position of each buoy j ($j = 1, \dots, n_B$), where n_B is the total number of buoys, scattered throughout the waterway or the shore, denoted as $(x_{B,j},\ y_{B,j})^\top$ is known, we can define a line, passing between two consecutive buoys $j,\ j+1$ as:

$$\mathcal{E}_j : \begin{cases} x'_{B,j}(b) = x_{B,j} + b\big(x_{B,j+1} - x_{B,j}\big), \\ y'_{B,j}(b) = y_{B,j} + b\big(y_{B,j+1} - y_{B,j}\big), \end{cases} \tag{12}$$

where $b \in [0, 1]$ is the path parameter, $(x'_{B,j}, y'_{B,j})^\top$ are the coordinates of each point that lies on $\mathcal{E}_j$. For each of the new future waypoints $k+1$ of the own vessel, we calculate its distance from $\mathcal{E}_j$ according to the following formula:

$$d_{W\mathcal{E}_j}(t) = \frac{\left|\delta x_{B,j}\left(y_{B,j} - y'_{k+1}(t)\right) - \left(x_{B,j} - x'_{k+1}(t)\right)\delta y_{B,j}\right|}{\sqrt{\delta x_{B,j}^2 + \delta y_{B,j}^2}}, \tag{13}$$

$\forall j \in \{1, 2, \dots, n_B\}$,

with $\delta x_{B,j} = x_{B,j+1} - x_{B,j}$ and $\delta y_{B,j} = y_{B,j+1} - y_{B,j}$ denoting the longitudinal and lateral distances between two consecutive buoys.

The clearance requirement to the waterway banks can then be mathematically translated as:

$$s_w w(x, y) \le d_{W\mathcal{E}_j}(t) \le (1 - s_w) w(x, y), \tag{14}$$

which after some algebraic manipulation renders the following constraints:

$$\left|\delta x_{B,j} \cdot \delta y_{k+1} - \delta y_{B,j} \cdot \delta x_{k+1}\right| \le (1 - s_w) w(x, y) \sqrt{\delta x_{B,j}^2 + \delta y_{B,j}^2} - \left|\delta x_{B,j}\left(y_{B,j} - y_{k+1}\right) - \left(x_{B,j} - x_{k+1}\right)\delta y_{B,j}\right|, \forall\ j = \{1, 2, \dots, n_B\}, \tag{15}$$

$$\left|\delta x_{B,j} \cdot \delta y_{k+1} - \delta y_{B,j} \cdot \delta x_{k+1}\right| \ge s_w w(x, y) \sqrt{\delta x_{B,j}^2 + \delta y_{B,j}^2} + \left|\delta x_{B,j}\left(y_{B,j} - y_{k+1}\right) - \left(x_{B,j} - x_{k+1}\right)\delta y_{B,j}\right|, \forall\ j = \{1, 2, \dots, n_B\}. \tag{16}$$

When the risk of collision exists for the own ASV described by (1) and it assumes a Give Way (GW) or Emergency Give Way (EGW) role, potential collisions with other vessels and the available infrastructure can be avoided, if the planned waypoints are horizontally and vertically displaced in the earth-fixed frame by $\delta x_{k+1}(t) \in \mathbb{R}$ and $\delta y_{k+1}(t) \in \mathbb{R}$, respectively, abiding by the constraints (11), (15) and (16). This implies a collision-free envelope for the own vessel, dependent on the traffic conditions and evolving over time, where the risk of collision is eliminated.

The various traffic rules also determine the specifics of the behavior that the vessels should adopt to avoid collisions. For instance, for head-on encounters, COLREGS mention that the vessels should take appropriate action to pass each other port to port. This can be translated in terms of a preference to the envelope as:

$$-(y_{k+1} - y_k) \cdot \delta x_{k+1} + (x_{k+1} - x_k) \cdot \delta y_{k+1} \le 0. \tag{17}$$

At each time t, the smallest possible path deviation would be preferred. This translates to an optimization problem, formulated as follows:

$$\min_{\delta x_{k+1}, \delta y_{k+1}} \left\{\delta x_{k+1}^2(t) + \delta y_{k+1}^2(t)\right\},\ \forall k = \{0, \dots, n-1\} \tag{18}$$

, subject to:

$$\text{Collision-free envelope} \begin{cases} \text{Eq. (11)},\ \forall i \in \{1, 2, \dots, n_v\}, \\ \text{Eq. (15)},\ \forall j \in \{1, 2, \dots, n_B\}, \\ \text{Eq. (16)},\ \forall j \in \{1, 2, \dots, n_B\}, \\ \text{Eq. (17)}. \end{cases}$$

4.2. Modular finite-state machine

In open and short-sea environments, where COLREGS are in effect, the traffic roles can be related to specific encounter situations, as (Tsolakis et al., 2024):

- GW: Head-On, Overtaking and Starboard-Crossing
- Stand-On (SO): Port-Crossing and Overtaken with no needed action
- EGW: Port-Crossing and Overtaken with emergency action

For inland waterway navigation, different traffic rules apply (i.e., BPR, PPR) and the relation between the traffic roles and encounter situations can change. For instance, according to Chapter 6 of BPR (Overheid.nl, 2025), the following different-to-COLREGS traffic rules apply:

- Head-on situation (Article 6.04): If two vessels are approaching each other on opposite courses in such a way that there is a risk of collision, the vessel not following the starboard side of the fairway shall give-way to the vessel following the starboard side of the fairway. If neither vessel follows the starboard side of the fairway, each shall give-way to vessels on the starboard side so that they pass each other port to port.
- Crossing situation (Article 6.17): If the courses of two ships cross each other in such a way that there is a risk of collision, the vessel not following the starboard side of the fairway shall give way to the vessel following the starboard side of the fairway. In case none of the ships follows the starboard side of the fairway, the ship approaching from the port side gives way to the vessel approaching from starboard side.

From the above, it is clear that the relation of the traffic role and the various encounter situations changes to:

- GW: Head-On (port side of the waterway), Overtaking and Crossing (port side of the waterway),
- SO: Head-On (starboard side of the waterway),Crossing (starboard side of the waterway) and Overtaken with no needed action,
- EGW: Crossing (starboard side of the waterway) and Overtaken with emergency action,

with the lane distance from the port and starboard side of the waterway, $d_l^{(p)}$ and $d_l^{(s)}$, the relative heading ψ_c and the relative bearing between the vessels ψ_β being important parameters for the role assignment.

The traffic role of the own vessel and other vessels can be determined using a Finite-State Machine (FSM) approach, such as the one shown in Fig. 3. When COLREGS are in effect, the design of the left hand side FSM in Fig. 3 has been already described in Tsolakis et al. (2024). Following a similar rationale, we construct the FSM corresponding to BPR traffic rules, and shown in the right hand side of Fig. 3. The following transition expressions of the FSM are proposed to determine the traffic role in this case:

$$\tilde{T}_{GW}^{ent} = T_{enc} \wedge \{T_{rsk} \wedge T_{bpr} \wedge [((T_{hdn} \vee T_{str}) \wedge \neg T_{stb}) \vee (T_{brn} \wedge (T_{ovr} \vee T_{stb}))]\}, \tag{19}$$

$$T_{GW}^{ext} = \neg T_{enc}, \tag{20}$$

$$T_{EM}^{ent} = T_{emg}, \tag{21}$$

$$T_{EM}^{ext} = \neg T_{emg}, \tag{22}$$

where the logic symbols $\wedge$, $\vee$, $\neg$ stand for "and", "or" and "not" respectively,

$$T_{\text{enc}} = d(t) < \rho_{\text{enc}}, \tag{23}$$

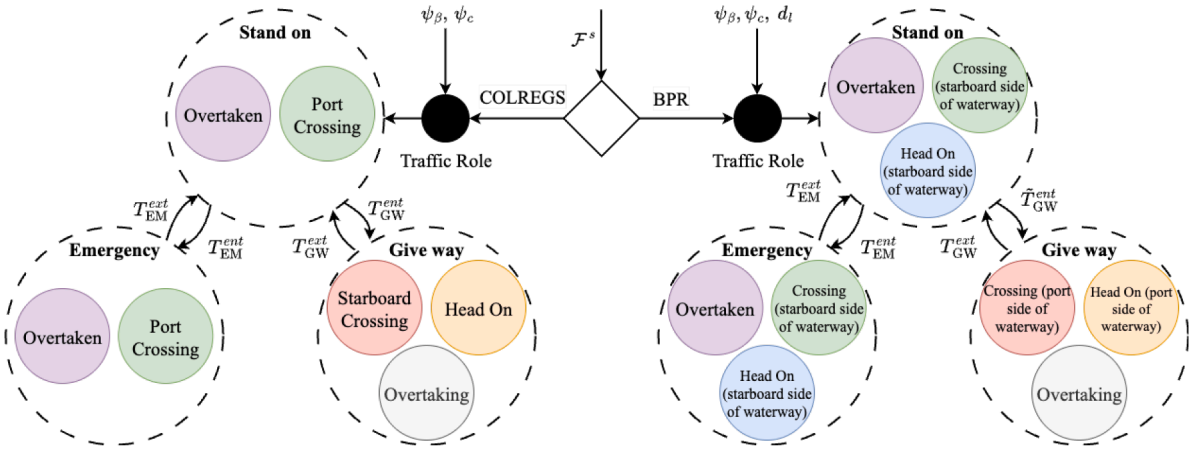

Fig. 3. Assignment of the traffic role using a modular Finite-State Machine Approach.

Algorithm 1 Collision-free Path Planner (at every timestep t).

Input: y_ζ, y_o, $\mathcal{F}$ ▷ Vessel sensor data, semantic database
Parameters: w, s_w ▷ waterway width, safety factor
Output: $\delta x_{k+1}(t), \delta y_{k+1}(t)$ ▷ Deviation of future planned waypoints

```
Calculate relative bearing ψ_β, and relative heading ψ_c between own vessel and vessel i, i = 1, 2, ..., n_v in ρ_enc   ▷ Tsolakis et al. (2024)
F^s ← Y_GPS × F using                                                                                                  ▷ Eq. (4)
Apply FSM in Fig. 3 to determine Traffic Role
if (Traffic Role is "GW") or (Traffic Role is"EGW") then
    k ← 1
    while k ≤ n − 1 do                                                                                                 ▷ n: number of waypoints
        (x, y) ↦ w
        Evaluate constraints (11), (15), (16), (17)
        Calculate δx_{k+1}, δy_{k+1} from (18)
        k ← k + 1
    end while
end if
```

$$T_{\text{rsk}} = d_{\text{CPA}}(t) < \rho_p + \rho_q + \rho_s, \tag{24}$$

$$T_{\text{bpr}} = d_l^{(s)} \geq d_l^{(p)} \tag{25}$$

$$T_{\text{hdn}} = (\psi_c(t) \geq \pi - \psi_h) \wedge (\psi_c(t) < \pi + \psi_h), \tag{26}$$

$$T_{\text{str}} = (\psi_c(t) \geq \pi + \psi_h) \wedge (\psi_c(t) < \frac{13\pi}{8}), \tag{27}$$

$$T_{\text{brn}} = (\psi_c(t) \geq \frac{13\pi}{8}) \wedge (\psi_c(t) < \frac{3\pi}{8}), \tag{28}$$

$$T_{\text{ovr}} = (\pi + \psi_\beta(t) - \psi_c(t) \geq \frac{5\pi}{8}) \wedge (\pi + \psi_\beta(t) - \psi_c(t) < \frac{11\pi}{8}), \tag{29}$$

$$T_{\text{stb}} = (\psi_\beta(t) \geq 0) \wedge (\psi_\beta(t) < \frac{5\pi}{8}), \tag{30}$$

$$T_{\text{emg}} = d(t) < \rho_{\text{emg}}, \tag{31}$$

with ρ_{emg} defining the radius of a circular area around the ASV within which, if a GW vessel enters, it is inferred it does not comply with the rules. The derived modular FSM considering both COLREGS and BPR is shown in Fig. 3. Online switching between the two branches is enabled through the use of a condition block activated by $\mathcal{F}^s$. Algorithm 1 outlines the integration of the traffic rule-aware role assignment by the FSM in Fig. 3 with the semantic reasoning capabilities of Section 4.1.

5. Simulation results

In this section, the results from the application of the collision-free path planner developed in Section 4 are presented. To this end, a Pusher-Barge ASV case study is employed, with dynamics described by (1) and (2), operating between a short-sea and a Dutch inland waterway environment. The prinicpal dimensions and parameters of the ASV model have been already provided in Zhang et al. (2025). A PID reference heading tracking controller is designed for path following, with the rudder angle δ updated for this purpose, as follows:

$$\delta(t) = K_p\left(\tilde{\psi}(t) + T_d\dot{\tilde{\psi}}(t) + \frac{1}{T_i}\int_0^t \tilde{\psi}(t)\right), \tag{32}$$

where $\tilde{\psi}(t) \triangleq \psi_{ref}(t) - \boldsymbol{y_\zeta}\{3\}(t)$ represents the heading angle tracking error at time step t, ψ_{ref} is calculated by the VS-LOS guidance law (Kougiatsos & Reppa, 2026), K_p is the controller's proportional gain, T_d and T_i are the derivative and integral time constants, respectively. The controller is tuned using a closed-loop natural frequency of $\omega_n = 0.1\ rad/s$ and a damping factor $\zeta = 0.95$ (Fossen, 2011). Since the measurements of the yaw rate r are not available, a command filter is used for its estimation (Farrell & Polycarpou, 2006). For simulation purposes, both the controller and the collision-free path planner are used with a sampling time $T_s = 1\ s$.

For the simulation purposes, the own vessel is tasked to follow a reference route starting at $(x, y) = (100, 0)^\top$ and finishing at $(x, y) = (5800, 0)^\top$, discretized in n evenly-spaced waypoints. The distance between waypoints is selected based on the Pusher-Barge vessel's advance distance, which is equal to 2.5 times the vessel's length (≅ 250 m) (Zhang et al., 2025). The waterway has a width w = 750 m (i.e., more than two times the length of the own vessel) and the safety clearance factor from the banks is taken as $s_w = 0.2$. Based on previous results of experiments related to ship-to-ship interaction (Vantorre et al., 2002), a minimum value for the safe distance ρ_s between the vessels equal to $0.5B$, where B is the own vessel's breadth, is assumed. This choice of value is shown to minimize the lateral force and yaw moment between the vessels during head-on and overtaking encounter situations. A value of $\rho_{enc} = 5L \approx 500$ m is assumed for the encounter distance of the own vessel. In order to semantically capture the effects of regulations in the path planner, Rules 6–8, 14, 16, 17, and 18 of COLREGS and Articles 6.03, 6.04, and 6.07 of BPR are semantically described in $\mathcal{F}$. The planner is tested in two scenarios. The first scenario involves head-on encounters, while the latter features crossing encounters. In each scenario, the own vessel transfers from a short-sea to an inland waterway environment. Based on the environment type at the time instant t, COLREGs or BPR may be used.

5.1. Head-on scenario

In this scenario, the own vessel encounters $n_v = 2$ opposite-moving Pusher-Barge vessels, posing risks for head-on collisions, as seen in Fig. 4. The encounter between the own vessel (blue) and vessel $i = 1$

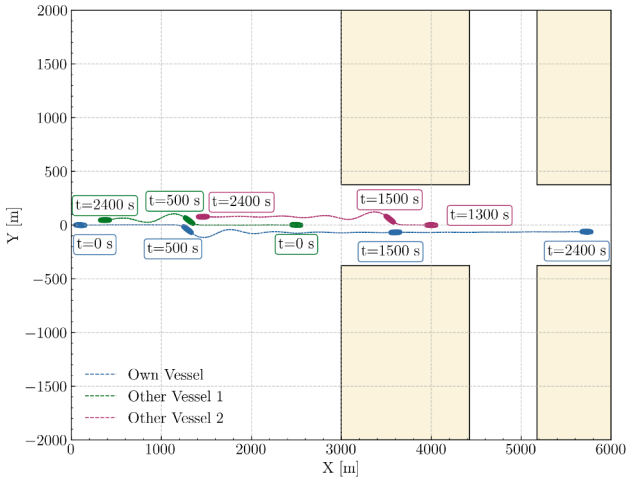

Fig. 4. Paths of the own (blue), other vessel $i = 1$ (green) and other vessel $i = 2$ (purple) on the X-Y plane for the head-on scenario. The geographic boundaries of the simulation map are denoted with yellow boxes. (For interpretation of the references to colour in this figure legend, the reader is referred to the web version of this article.)

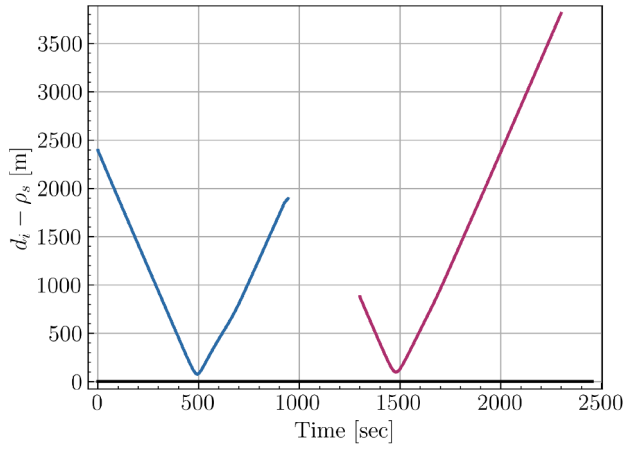

Fig. 5. Distance between the own vessel and other vessel $i = 1$ (d_1 shown in blue), and between the own vessel and other vessel $i = 2$ (d_2 shown in purple), during each head-on encounter. (For interpretation of the references to colour in this figure legend, the reader is referred to the web version of this article.)

(green) occurs at the short-sea environment, where the other vessel $i = 1$ starts from the point $(x_{o,1}, y_{o,1}) = (2500, 0)^\top$. The encounter between the own vessel and vessel $i = 2$ (purple) occurs in the Dutch Inland waterway environment, where the other vessel $i = 2$ starts from the point $(x_{o,2}, y_{o,2}) = (4000, 0)^\top$. The path of each vessel over time, the timestamps corresponding to specific events (e.g., start and end point of each vessel, points where the vessels are at the closest distance), as well as the geographical bounds used in the simulation are shown in Fig. 4. From the same Figure, the distances $d_l^{(p)}$ and $d_l^{(s)}$ of each vessel from the banks of the inland waterway can also be inferred.

Fig. 5 illustrates the difference between the achieved distance between the own vessel and vessel $i \in \{1, 2\}$, denoted as d_i and the safe distance ρ_s. More specifically, the difference $d_1 - \rho_s$ is shown with a blue color, while the difference $d_2 - \rho_s$ is shown with a purple color. Both curves receive values greater than 0, which signifies that vessels keep well-clear from each other, respecting the safe distance.

Fig. 6 illustrates the time histories of the heading angles corresponding to the three simulated vessels for the case study. During the first encounter, the own vessel (blue) and other vessel $i = 1$ (green) both make evasive maneuvers to avoid collision, as seen in Fig. 4. Thus, the heading measurement $\boldsymbol{y}_{\boldsymbol{\zeta}}\{3\}$ drops below 0 deg (turn to starboard), while $\psi_{o,1}$ assumes values between 180 and 150 deg (turn to starboard) in Fig. 6. As a result, the two vessels pass each other port to port, in accordance to COLREGs, before starting to correct their headings again to their original values, as shown in Fig. 4. The own vessel continues with almost zero heading in the inland waterway environment (see Fig. 6), where it encounters the other vessel $i = 2$ (purple) coming from the opposite direction. According to Fig. 4, the distance of the own vessel from the starboard side bank is less than the distance of the other vessel $i = 2$ from the same bank. As a result, the own vessel follows the starboard side of the waterway. Based on Rule 6.04 of BPR, the modular FSM in Fig. 3 assigns the Stand-On role to the own vessel. Symmetrically, the other vessel $i = 2$ assumes a Give-Way role and should take action to avoid collision. The appropriate action for vessel $i = 2$ is to alter its reference path in such a way as to pass the own vessel port to port, illustrated by the reduction of the heading angle between 180 deg and 150 deg (turn to starboard) in Fig. 6. The own vessel proceeds on its original path, without an action required to avoid collision. Thus, the two vessels resolve the second head-on encounter scenario in accordance to the BPR rules, as illustrated in Fig. 4.

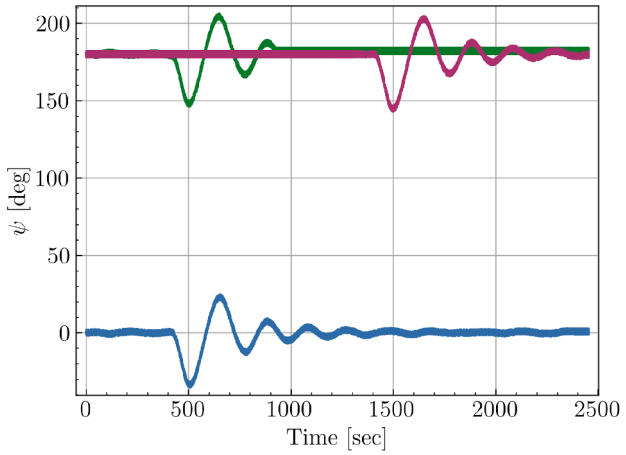

Fig. 6. Time history of the recorded heading angles for the own vessel (blue), other vessel $i = 1$ (green), and other vessel $i = 2$ (purple), in the examined head-on scenario. (For interpretation of the references to colour in this figure legend, the reader is referred to the web version of this article.)

5.2. Crossing scenario

For the second scenario, illustrated in Fig. 7, the own vessel encounters $n_v = 2$ Pusher-Barge vessels, crossing from a $-150\ deg$ and $90\ deg$ angle, respectively. The encounter between the own vessel (blue) and vessel $i = 1$ (green) occurs at the short-sea environment, where the other vessel $i = 1$ starts from the point $(x_{o,1}, y_{o,1}) = (2495.7, 575)^\top$. The encounter between the own vessel and vessel $i = 2$ (purple) occurs in the Dutch Inland waterway environment, where the other vessel $i = 2$ starts from the point $(x_{o,2}, y_{o,2}) = (4750, -700)^\top$. The path of each vessel over time, the timestamps corresponding to specific events (e.g., start and end point of each vessel, points where the vessels are at the closest distance), as well as the geographical bounds used in the simulation are shown in Fig. 7. From the same Figure, the distances $d_l^{(p)}$ and $d_l^{(s)}$ of each vessel from the banks of the inland waterway can also be inferred.

Fig. 8 illustrates the difference between the achieved distance between the own vessel and vessel $i \in \{1, 2\}$, denoted as d_i and the safe distance ρ_s. More specifically, the difference $d_1 - \rho_s$ is shown with blue colored line, while the difference $d_2 - \rho_s$ is shown with a purple colored line. Again, both curves remain positive, which signifies that vessels stay

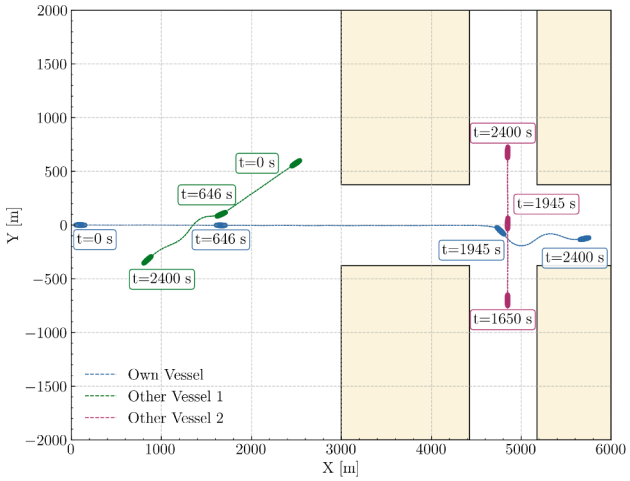

Fig. 7. Paths of the own (blue), other vessel $i = 1$ (green) and other vessel $i = 2$ (purple) on the X-Y plane for the crossing scenario. The geographic boundaries of the simulation map are denoted with yellow boxes. (For interpretation of the references to colour in this figure legend, the reader is referred to the web version of this article.)

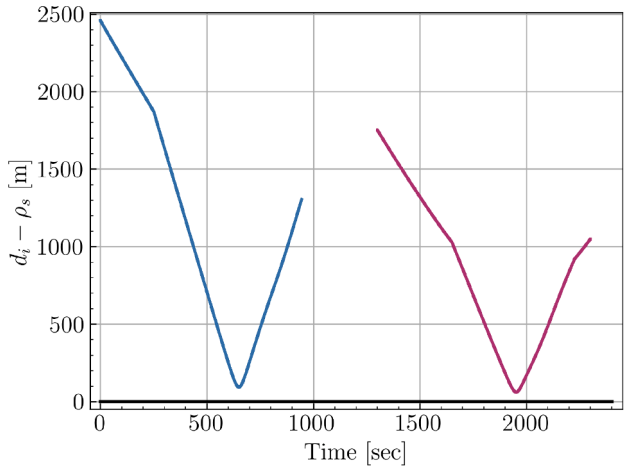

Fig. 8. Distance between the own vessel and other vessel $i = 1$ (d_1 shown in blue), and between the own vessel and other vessel $i = 2$ (d_2 shown in purple), during each crossing encounter. (For interpretation of the references to colour in this figure legend, the reader is referred to the web version of this article.)

clear from each other, respecting the safe distance. The time windows of the two head-on encounters are highlighted, based on the defined ρ_{enc}.

Fig. 6 illustrates the time histories of the heading angles corresponding to the three simulated vessels for the case study. From the own's vessel's perspective, the encounter scenario with the other vessel $i = 1$ is perceived as a port crossing situation, and, according to the FSM in Fig. 3, the stand-on role is assumed. Similarly, the other vessel $i = 1$ assumes a give-way role and is required to alter its course to avoid collision. In Fig. 7, the own vessel (blue) indeed stands on its path, while the crossing vessel $i = 1$ makes an evasive maneuver to avoid collision. During this maneuver, $\psi_{o,1}$ assuming values between -180 and -150 deg, according to Fig. 9. As a result, the other vessel $i = 1$ crosses behind the own vessel, and then returns to its original path. The own vessel continues with almost 0 deg heading in the inland waterway environment, where it meets the other vessel $i = 2$ (purple) crossing at a 90 deg angle, as seen in Fig. 7. According to the same Figure, the distance of the own vessel from the starboard side bank is bigger than the distance of the other vessel $i = 2$ from its respective starboard side bank. As a result, the other vessel $i = 2$ is the one following the starboard side of the

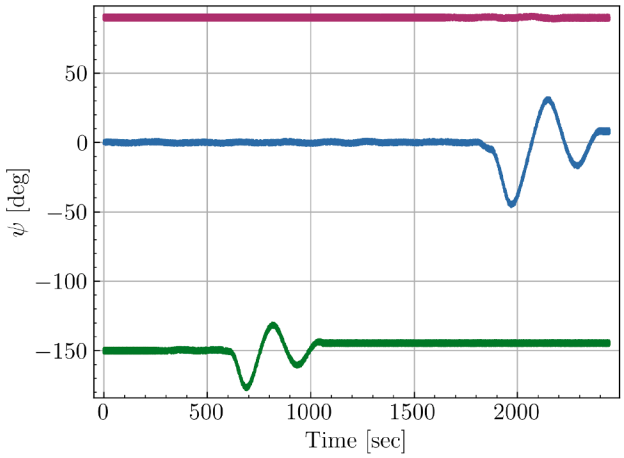

Fig. 9. Time history of the recorded heading angles for the own vessel (blue), other vessel $i = 1$ (green), and other vessel $i = 2$ (purple), in the examined crossing scenario. (For interpretation of the references to colour in this figure legend, the reader is referred to the web version of this article.)

waterway, and the own vessel should give way according to the BPR branch of the FSM in Fig. 3. The appropriate action for the own vessel is to alter its reference path and cross behind the other vessel $i = 2$. This is illustrated by the reduction of the heading angle between 0 deg and -50 deg in Fig. 9. The own vessel returns to its original path, after the encounter scenario has been resolved. The other vessel $i = 2$ has no need to alter its heading, as illustrated with the purple line in Fig. 9. Thus, the two vessels resolve the crossing scenario in accordance to the BPR rule 6.17, as shown in Fig. 7.

6. Conclusion

This paper presented an intelligent guidance scheme enabling collision-free navigation of vessels across diverse operational environments. By integrating semantic knowledge with quantitative sensor data, the framework was able to support rule-aware and context-sensitive decision-making, accounting for traffic interactions with both other vessels and the surrounding infrastructure. The multi-environment head-on and crossing encounter scenarios demonstrated the framework's capability to adapt seamlessly to varying regulatory requirements, ensuring rule-aware collision avoidance behavior while maintaining the required safe distances and clearances.

Dealing with more complex scenarios (e.g., high traffic) will impact the decision-making of the collision-free path planner, in terms of the calculation of the collision-free envelope using (11), (15), (16), and (17). As such, future research will focus on the stress testing of the developed algorithm in a multitude of encounter scenarios. A more thorough design of the control system is required to ensure that the vessel is able to follow the path deviations suggested by the planner, under the influence of disturbances and faults. The inclusion of the propeller speed as a control input, and of the safe speed as a constraint in the path planner, is crucial in this respect.

CRediT authorship contribution statement

Nikos Kougiatsos: Writing – original draft, Writing – review & editing, Visualization, Validation, Software, Methodology, Investigation, Formal analysis, Data curation, Conceptualization; **Abhishek Dhyani:** Writing – original draft, Writing – review & editing, Software, Methodology; **Vasso Reppa:** Writing – review & editing, Supervision, Project administration, Funding acquisition.

Declaration of competing interest

The authors declare the following financial interests/personal relationships which may be considered as potential competing interests: Vasso Reppa reports financial support was provided by European Union Horizon 2020 research and innovation programme. If there are other authors, they declare that they have no known competing financial interests or personal relationships that could have appeared to influence the work reported in this paper.

Funding

The research leading to these results has received funding from the European Union's Horizon 2020 research and innovation programme grant agreement No. 101096923 (SEAMLESS Project). This publication reflects only the authors' view, exempting the European Union and the granting authority from any liability. Project website: https://www.seamless-project.eu/.

Supplementary material

Supplementary material associated with this article can be found in the online version at 10.1016/j.conengprac.2026.107113.

References

Ali, H., Xiong, G., Tianci, Q., Kumar, R., Dong, X., & Shen, Z. (2024). Autonomous ship navigation with an enhanced safety collision avoidance technique. *ISA Transactions*, *144*, 271–281. https://doi.org/10.1016/j.isatra.2023.10.019

Commission Centrale pour la Navigation du Rhin (CCNR) (2024). Règlement de police pour la navigation du rhin (RPNR). Technical Report État.

European Maritime Safety Agency (2024). Annual overview of marine casualties and incidents 2024. Technical Report European Maritime Safety Agency.

Farrell, J. A., & Polycarpou, M. M. (2006). Adaptive approximation based control: Unifying neural, fuzzy and traditional adaptive approximation approaches. John Wiley & Sons.

Fossen, T. I. (2011). Handbook of marine craft hydrodynamics and motion control. John wiley & sons.

He, Y., Liu, X., Zhang, K., Mou, J., Liang, Y., Zhao, X., Wang, B., & Huang, L. (2022). Dynamic adaptive intelligent navigation decision making method for multi-object situation in open water. *Ocean Engineering*, *253*, 111238.

He, Y., Zou, L., Wu, Z.-X., Liu, S.-Y., Chen, W.-M., Zou, Z.-J., & Celik, C. (2025). Integrated path following and collision avoidance control for an underactuated ship based on MFAPC. *Ocean Engineering*, *324*, 120706.

Hinostroza, M. A., Xu, H., & Guedes Soares, C. (2021). Motion planning, guidance, and control system for autonomous surface vessel. *Journal of Offshore Mechanics and Arctic Engineering*, *143*(4), 041202.

International Maritime Organization (IMO) (1972). Convention on the international regulations for preventing collisions at sea, 1972 (COLREG). International Maritime Organization (IMO) London, UK (consolidated edition (as amended) ed.). Adopted 20 October 1972; entered into force 15 July 1977.

Johansen, T. A., Perez, T., & Cristofaro, A. (2016). Ship collision avoidance and COLREGS compliance using simulation-based control behavior selection with predictive hazard assessment. *IEEE Transactions on Intelligent Transportation Systems*, *17*, 3407–3422. https://doi.org/10.1109/TITS.2016.2551780

Kougiatsos, N., & Reppa, V. (2026). Virtual sensor-informed motion planning for safe autonomous waterborne navigation. To appear in the proceedings of the transport research arena 2026, Budapest, Hungary.

Kougiatsos, N., Scheffers, E. L., van Benten, M. C., Schott, D. L., de Vos, P., Negenborn, R. R., & Reppa, V. (2025). An intelligent agent-based resilient framework for marine vessel mission adaptations. *IEEE Open Journal of Intelligent Transportation Systems*, (pp. 1–1). https://doi.org/10.1109/OJITS.2025.3539419

Lataire, E., Vantorre, M., & Delefortrie, G. (2018). The influence of the ship's speed and distance to an arbitrarily shaped bank on bank effects. *Journal of Offshore Mechanics and Arctic Engineering*, *140* 021304.

Li, J., Peng, Z., Liu, L., Wang, D., Wang, A., & Gu, N. (2023). Safety-critical line-of-sight path following guidance of an under-actuated maritime autonomous surface ship based on robust optimization. In *2023 42nd Chinese control conference (CCC)* (pp. 2988–2993). IEEE.

Luo, J., Geng, X., Li, Y., & Yu, Q. (2022). Study on the risk model of the intelligent ship navigation. *Wireless Communications and Mobile Computing*, *2022*(1), 3437255.

Overheid.nl (2025). Binnenvaartpolitiereglement. https://wetten.overheid.nl/BWBR0003628/2025-01-01.

Pratson, L. F. (2023). Assessing impacts to maritime shipping from marine chokepoint closures. *Communications in Transportation Research*, *3*. https://doi.org/10.1016/j.commtr.2022.100083

Smeds, E., & Cavoli, C. (2021). *Pathways for accelerating transitions towards sustainable mobility in European cities*. Barcelona Centre for International Affairs (CIDOB).

Tran, H. A., Lauvås, N., Johansen, T. A., & Negenborn, R. R. (2025). Asynchronous distributed collision avoidance with intention consensus for inland autonomous ships. arXiv preprint arXiv:2501.15899.

Tsolakis, A., Negenborn, R. R., Reppa, V., & Ferranti, L. (2024). Model predictive trajectory optimization and control for autonomous surface vessels considering traffic rules. *IEEE Transactions on Intelligent Transportation Systems*, *25*(8), 9895–9908.

Vantorre, M., Verzhbitskaya, E., & Laforce, E. (2002). Model test based formulations of ship-ship interaction forces. *Ship Technology Research*, *49*(3), 124–141.

Yang, T., Han, C., Qin, M., & Huang, C. (2019). Learning-aided intelligent cooperative collision avoidance mechanism in dynamic vessel networks. *IEEE Transactions on Cognitive Communications and Networking*, *6*(1), 74–82.

Yoshioka, H., & Hashimoto, H. (2022). AI-based collision avoidance for automatic ship navigation. In *Proceedings of the 18th international ship stability workshop* (pp. 229–234).

Yoshioka, H., Hashimoto, H., & Matsuda, A. (2024). Artificial intelligence for cooperative collision avoidance of ships developed by multi-agent deep reinforcement learning. In *International conference on offshore mechanics and arctic engineering* (p. V006T08A036). American Society of Mechanical Engineers (*vol. 87844*).

Zhang, C., Dhyani, A., Ringsberg, J. W., Thies, F., Negenborn, R. R., & Reppa, V. (2025). Nonlinear model predictive control for path following of autonomous inland vessels in confined waterways. *Ocean Engineering*, *334*, 121592.

Zhou, H., Ren, Z., Marley, M., & Skjetne, R. (2022). A guidance and maneuvering control system design with anti-collision using stream functions with vortex flows for autonomous marine vessels. *IEEE Transactions on Control Systems Technology*, *30*(6), 2630–2645.

Zhou, Z., Zhang, Y., & Wang, S. (2021). A coordination system between decision making and controlling for autonomous collision avoidance of large intelligent ships. *Journal of Marine Science and Engineering*, *9*(11), 1202.